

# Inference Method for Residual Stress Field of Titanium Alloy Parts Based on Latent Gaussian Process Introducing Theoretical Prior

CHEN Junsong<sup>1</sup>, LIU Changqing<sup>1\*</sup>, ZHAO Zhiwei<sup>1</sup>, WANG Wei<sup>2</sup>,  
XIANG Bingfei<sup>3</sup>, WEI Zhenkun<sup>3</sup>, LI Yingguang<sup>1</sup>

1. College of Mechanical and Electrical Engineering, Nanjing University of Aeronautics and Astronautics, Nanjing 210016, P. R. China; 2. School of Engineers Science, University of Skövde, Skövde, Sweden;  
3. Hong Du Aviation Industry Group Ltd, Nanchang 330096, P. R. China

(Received 23 October 2023; revised 29 February 2024; accepted 15 March 2024)

**Abstract:** Residual stress (RS) within titanium alloy structural components is the primary factor contributing to machining deformation. It comprises initial residual stress (IRS) and machined surface residual stress (MSRS), resulting from the interplay between IRS and high-level machining-induced residual stress (MIRS). Machining deformation of components poses a significant challenge in the aerospace industry, and accurately assessing RS is crucial for precise prediction and control. However, current RS prediction methods struggle to account for various uncertainties in the component manufacturing process, leading to limited prediction accuracy. Furthermore, existing measurement methods can only gauge local RS in samples, which proves inefficient and unreliable for measuring RS fields in large components. Addressing these challenges, this paper introduces a method for simultaneously estimating IRS and MSRS within titanium alloy aircraft components using a Bayesian framework. This approach treats IRS and MSRS as unobservable fields modeled by Gaussian processes. It leverages observable deformation force data to estimate IRS and MSRS while incorporating prior correlations between MSRS fields. In this context, the prior correlation between MSRS fields is represented as a latent Gaussian process with a shared covariance function. The proposed method offers an effective means of estimating the RS field using deformation force data from a probabilistic perspective. It serves as a dependable foundation for optimizing subsequent deformation control strategies.

**Key words:** titanium alloy; residual stress field inference; latent Gaussian process; machining deformation

**CLC number:** V262.3

**Document code:** A

**Article ID:** 1005-1120(2024)02-0135-12

## 0 Introduction

Large structural components are extensively utilized in the aerospace industry. Titanium alloys are progressively replacing aluminum alloys as vital load-bearing components and essential connections in modern aircraft due to their exceptional mechanical properties.

The latest generation of aircraft aims for peak overall performance<sup>[1]</sup>. Titanium structural components, which form the aircraft's framework, de-

mand shorter production cycles and heightened manufacturing precision. This poses a distinct challenge in terms of controlling machining deformation.

Research has indicated that the residual stress (RS) field, consisting of initial residual stress (IRS) and machined surface residual stress (MSRS), is the primary contributor to machining deformation. IRS represents the mechanical stress retained within the bulk material, achieving self-equilibrium while satisfying static force and moment equilibrium conditions. MSRS, on the other hand, is the residual

\*Corresponding author, E-mail address: liuchangqing@nuaa.edu.cn.

**How to cite this article:** CHEN Junsong, LIU Changqing, ZHAO Zhiwei, et al. Inference method for residual stress field of titanium alloy parts based on latent Gaussian process introducing theoretical prior[J]. Transactions of Nanjing University of Aeronautics and Astronautics, 2024, 41(2): 135-146.

<http://dx.doi.org/10.16356/j.1005-1120.2024.02.001>

stress formed within the top 0.2 mm depth near the machined surface due to the interplay of IRS and the introduced additional machining-induced residual stress (MIRS) under cutting force and thermal effects. Yang et al.<sup>[2]</sup> have identified IRS and MSRS as the principal factors behind machining deformation in titanium alloy structural components. Wang et al.<sup>[3]</sup> have demonstrated that the impact of IRS and MSRS on total deformation depends on the component's stiffness. In cases of relatively high stiffness, IRS-induced machining deformation accounts for 90% of the total deformation. However, as the component's stiffness decreases, MSRS assumes a dominant role, accounting for 47.1%. Hence, accurately inferring both IRS and MSRS is crucial for predicting deformation and guiding deformation control, ultimately enhancing the overall aircraft performance.

Zhao et al.<sup>[4]</sup> proposed a method for inferring IRS field using deformation force, which is an inverse problem and the Tikhonov regulation (TR) method was used to reduce the impact of measurement noise on the accuracy of the inference results by constraining the magnitude and stability of the so-

lution. However, inferring IRS and MSRS simultaneously constitutes a multi-source inverse problem. The traditional TR method, when employed to solve the problem, are prone to falling into local minima of the objective function, making it challenging to ensure the accuracy.

In addressing the above issue, this paper introduces a Bayesian model for inferring the RS field of titanium alloy parts based on latent Gaussian process (GP) as illustrated in Fig.1. The advantage of Bayesian model is to efficiently integrate various prior information into the problem. The latent GPs are used to model unobservable IRS and MSRS and accurately capture the theoretical correlation between MSRS on different machined surfaces by introducing a kernel function with shared covariance, which helps to reduce the number of parameters and improve the accuracy of inference results. The remainder of the paper is structured as follows: Section 1 presents related work, Section 2 details the methodology, and Section 3 provides a numerical example validating the methodology. Finally, key conclusions are summarized in Section 4.

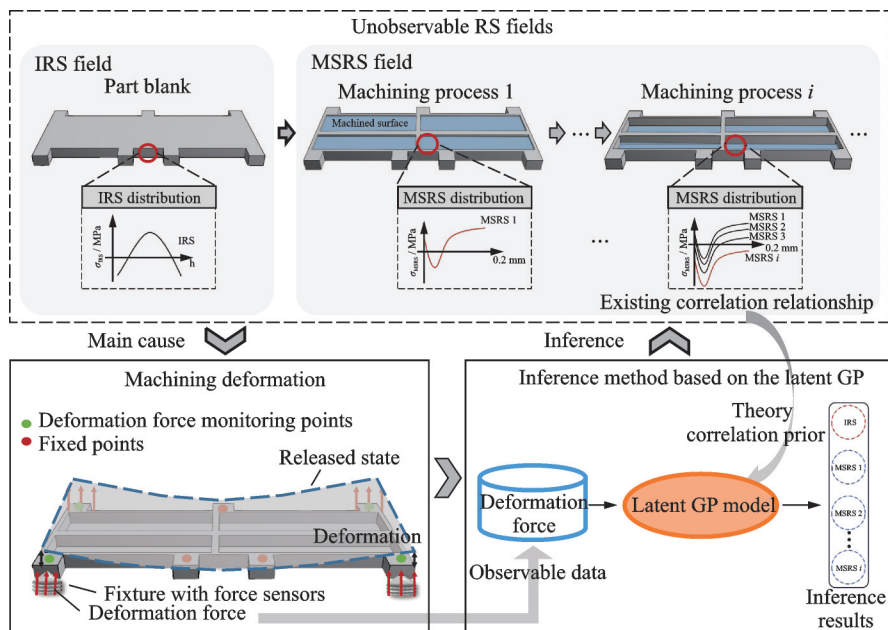


Fig.1 Schematic diagram of RS field inference method based on latent GP

## 1 Related Work

Existing methods for obtaining RS fields mainly include RS prediction and measurement method.

### 1.1 RS prediction method

The prediction of IRS primarily involves simulating the blank preparation processes, including

forging, rolling, and heat treatment, through numerical simulations<sup>[5]</sup> to estimate the IRS after blank forming. However, the formation of the RS field in the blank is a complex interplay of mechanical and thermal factors, whereas simulation processes can only account for certain influencing factors. Constitutive and interfacial heat transfer models are hypothesized, simplified, and approximated, resulting in discrepancies between RS field predictions and actual outcomes.

Methods for predicting MIRS primarily fall into two categories: Analytical and numerical approaches. Analytical methods establish mapping models between physical parameters and the MIRS field, such as cutting parameters, cutting heat, and cutting force. Shan et al.<sup>[6]</sup> proposed an analytical model for predicting orthogonal cutting stress by considering cutting force and cutting heat, while Cheng et al.<sup>[7]</sup> introduced an analytical model for MIRS prediction based on GP regression. Analytical methods offer swift computations but pose challenges in ensuring high accuracy. On the other hand, numerical methods simulate the cutting process involving both the tool and the workpiece to predict the MIRS field generated by force-thermal coupling during machining. Yang et al.<sup>[8]</sup> proposed a dynamic mesh refinement algorithm to balance speed and accuracy in the three-dimensional finite element simulation model. Styger et al.<sup>[9]</sup> investigated the influence of constitutive model parameters on the prediction results of Ti6Al4V using numerical calculations.

Existing methods for predicting residual stress fields through simulating material forming processes offer a general overview of RS field distribution trends. However, owing to the intricacies of the raw material forming process, these methods frequently necessitate multiple assumptions, simplifications, and approximations during the modeling and solving stages.

## 1.2 RS measurement method

RS measurement methods can be categorized into destructive and non-destructive techniques.

The destructive method involves physically or chemically altering materials to release RS in specif-

ic regions. The RS in the material region is then calculated by measuring the strain or displacement caused by local changes in RS. Destructive methods primarily include the drilling method<sup>[10]</sup>, the crack compliance method<sup>[11]</sup>, the layer removal method<sup>[12]</sup>, and the contour method<sup>[13]</sup>. However, these destructive measurement methods result in stress release during the measurement process, leading to the redistribution of RS within the components and the accumulation of measurement errors, thus resulting in inaccurate RS measurements.

Non-destructive methods include X-ray diffraction, neutron diffraction<sup>[14]</sup>, and ultrasonic testing<sup>[15]</sup>, which allow for RS calculations in materials without causing damage or affecting the usability of the object. Currently, the most frequently employed non-destructive method for RS detection is X-ray diffraction, which can measure surface stresses within a depth of 5  $\mu\text{m}$  to 20  $\mu\text{m}$ <sup>[16]</sup>.

In the case of titanium alloy structural components, the IRS field is complex, and additional high-level MIRS is introduced during the machining process. Even within the same batch of materials, significant differences in RS distributions can exist. Existing RS prediction methods struggle to account for the numerous uncertain factors during material forming processes, resulting in limited accuracy in predicting residual stress fields. Moreover, residual stress measurement methods are limited to local measurements, which can be inefficient and inaccurate. Consequently, existing methods face challenges in meeting the requirements for accurately predicting and controlling deformation in machining processes.

To achieve accurate RS inference, based on the author team research<sup>[4]</sup>, this paper proposes a method to infer unobservable IRS and MSRS using monitored deformation force.

## 2 Methodology

Although directly measuring the RS field can be challenging, there are quantifiable physical parameters within the manufacturing process that represent the impact of RS on deformation, such as de-



workpiece, the above equation can be decomposed as follows

$$[M_{IRS} \ M_{MSRS}] \begin{bmatrix} \sigma_{IRS} \\ \sigma_{MSRS} \end{bmatrix} = F_c \quad (4)$$

where  $M_{IRS}$  and  $M_{MSRS}$  are the corresponding volume coefficient matrices of the IRS and MSRS, respectively. The value in the volume coefficient matrix is the influence coefficient of the unit RS in each area on the deformation force at each measurement point under the current geometric state of the part, which can be calculated by finite element analysis.  $\sigma_{IRS}$  and  $\sigma_{MSRS}$  are the residual stress fields of the IRS and MSRS, respectively.  $F_c$  is the deformation force of all measuring points under the current geometric state of the part. Measured by the fixture with an integrated force sensor is located at the measurement point.

## 2.2 Finite element simulation of MSRS

Finite element modeling (FEM) technology has proven to be a highly effective approach for simulating metal processing procedures. It enables the analysis of cutting parameters such as force, temperature, residual stress, and chip formation during the cutting process. In the pursuit of understanding the distribution patterns of MSRS, this paper employs FEM to simulate and analyze MSRS in Ti6Al4V.

Yue et al.<sup>[17]</sup> demonstrated that during the planar milling, under identical process parameters, the simulation results from two-dimensional orthogonal cutting can provide valuable references for predicting trends and patterns in actual milling outcomes. As illustrated in Fig.3, to streamline computation and simplify geometric construction, this paper has developed a condensed two-dimensional cutting model within the ABAQUS/Explicit software. It simulates the machining process through explicit, dynamic, and the temperature-displacement coupling analysis.

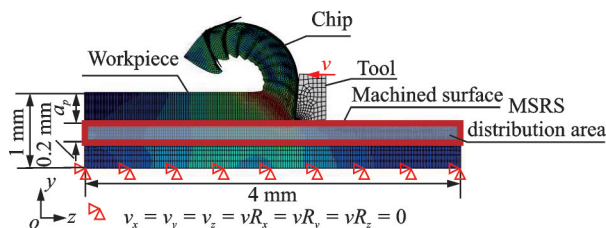


Fig.3 Initial geometry and boundary conditions of the model

The simulation parameters are as follows: The workpiece material is Ti6Al4V, the tool material is YG6X, the rake angle of the tool is  $4^\circ$ , and the clearance angle is  $10^\circ$ . And it is set as a rigid body, with a feed rate  $f$  of 0.1 mm/r, a cutting speed  $v$  of 100 m/min, and a depth of cut  $a_p$  of 0.4 mm.

Based on the actual machining process, the model sets up three analysis steps: Cutting (feed), unloading (retraction) and cooling. The air-cooling process of the workpiece is simulated by the heat exchange analysis step of the workpiece, tool, and air. The IRS is applied to the workpiece by defining a predefined field, and the trends of MSRS after coupling under different IRS fields are predicted.

The material constitutive model of Ti6Al4V is the Johnson-Cook (JC) model<sup>[18]</sup>, as shown in

$$\sigma = [A + B\epsilon^n] \times \left[ 1 + C \ln \left( \frac{\dot{\epsilon}}{\dot{\epsilon}_0} \right) \right] \times \left[ 1 - \left( \frac{T - T_r}{T_m - T_r} \right)^m \right] \quad (5)$$

where  $\sigma$  is the equivalent stress,  $\epsilon$  the equivalent plastic strain,  $\dot{\epsilon}$  the equivalent strain rate,  $\dot{\epsilon}_0$  the reference strain rate,  $A$  the initial yield stress,  $B$  the modulus of elasticity,  $n$  the strain hardening coefficient,  $C$  the strain rate dependent coefficient, and  $m$  is the thermal softening coefficient;  $T_m$  and  $T_r$  are the melting temperature of the room temperature and the workpiece material. The JC parameters, workpiece and tool material properties used in this paper are given in Ref.[19].

The predicted MSRS results from the FE model are compared with the actual residual stress values measured by X-ray diffraction under the same machining parameters, validating the effectiveness of the established model. The FE model prediction result is compared with the RS values measured by X-ray diffraction method to verify the effectiveness of the established model. The result is shown in Table 1.

Comparing with the measured MSRS values, the error of FE model prediction results in the  $x$  direction is 4.2%, and the error of prediction results in the  $y$  direction is 4.7%, which is within a reasonable range and can verify the accuracy of the FE

**Table 1 Comparison of prediction and measurement results**

MSRS	$x$ direction /MPa	$y$ direction/MPa
Predicted	-253.47	-343.23
Measured	-243.1	-360.15
Prediction error/%	4.2	4.7

model in this study.

To investigate the distribution of the MSRS with consistent processing parameters but varying IRS values, whose values in the  $x$  direction were selected based on the empirical knowledge. These values were  $-175$ ,  $-125$ ,  $-75$ ,  $-50$ ,  $-25$ ,  $0$ ,  $25$ ,  $50$ ,  $75$ ,  $125$ , and  $175$  MPa, respectively.

The MSRS is distributed within a depth range of  $0.2$  mm from the surface layer<sup>[19]</sup>. Based on the simulation results, the stress values in the  $x$  direction of  $100$  element nodes per layer were extracted in MSRS distributed area. And their average was calculated to characterize the RS value of the current layer, which allowed us to understand the overall trend of MSRS distribution in the depth direction of the MSRS distributed area.

According to the results, the through-thickness MSRS of different IRS values have similar profiles, which exhibit a “ $\surd$ ” distribution pattern, but different magnitude as illustrated in Fig.4. The surface of the MSRS is initially compress. With the increase of depth, MSRS decreases first, reaches the maximum magnitude, and then gradually increases, reaching the tensile state and balanced state. It is found that the magnitudes of MSRS depend on the IRS values

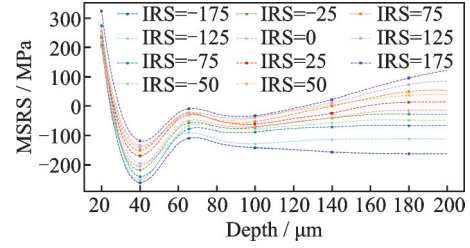


Fig.4 Distribution of MSRS of different IRS values

set in the workpiece region by analyzing the magnitude of MSRS stress values at key trend points, such as points at the depth of  $40$ ,  $65$ , and  $180$   $\mu\text{m}$ . As the values of IRS set as predefined field increase, the MSRS value level continues to increase, which validates a direct correlation between magnitudes of MSRS and the values of IRS.

### 2.3 Inference method for RS fields based on latent GP

The acquisition of the RS field remains a global challenge. In response to this challenge, this paper introduces an inference method based on the latent GP within a Bayesian framework as illustrated in Fig.5. This approach is well-suited for addressing inverse probability problems, utilizing observable data, and incorporating prior knowledge. In the proposed method, the monitoring data of deformation forces during the machining process are considered as observable data. The multiple unobservable and unmeasurable IRS and MSRS fields are treated as outputs of a latent vector-valued GP, employing a shared covariance function to capture correlations between these related outputs.

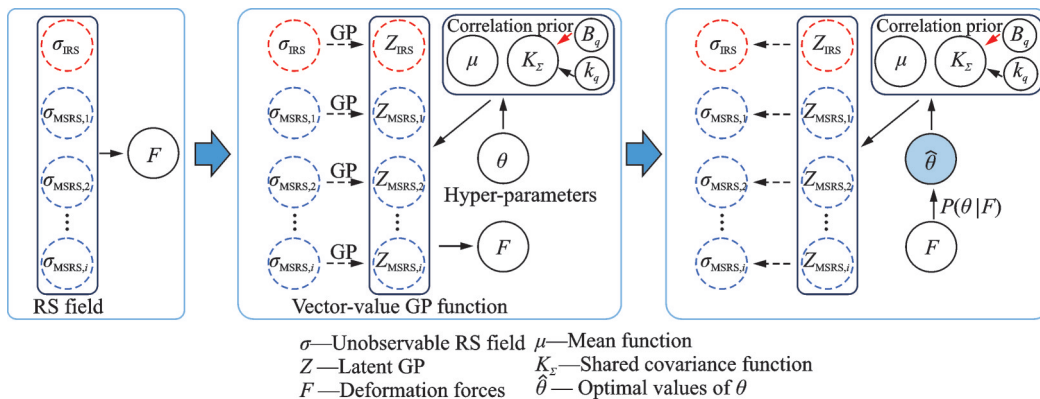


Fig.5 Graphical representation of RS field inference method

Building upon the mechanical relationship established in Section 2.1, it is evident that deforma-

tion force is a function of IRS and MSRS. Consequently, the RS inference is transformed into the

task of inferring unobservable latent RS fields using observable deformation force data. Within the Bayesian framework, latent GPs are employed to represent the unobservable IRS field and multiple MSRS fields as priors, as demonstrated in

$$\sigma_{\text{IRS}} \sim GP(\tilde{\sigma}_{\text{IRS}}, \mathbf{K}_{\text{IRS}}) \quad (6)$$

$$\sigma_{\text{MSRS},i} \sim GP(\tilde{\sigma}_{\text{MSRS},i}, \mathbf{K}_{\text{MSRS},i}) \quad i = 1, 2, \dots, N \quad (7)$$

where  $\sigma_{\text{IRS}}$  and  $\sigma_{\text{MSRS},i}$  are the IRS field and the  $i$ th MSRS field in Fig.5;  $\tilde{\sigma}$  is a prior to the mean residual stress, and  $\mathbf{K}$  the covariance of each RS field. The position relationship between various MSRS and IRS fields is illustrated in Fig.6.

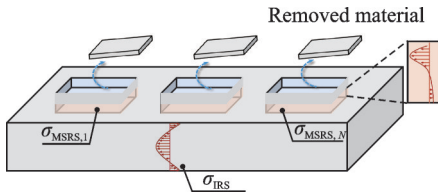


Fig.6 Position relationship between various MSRS and IRS fields

To introduce the correlation prior between MSRS, a latent vector-valued function GP with a shared covariance function is modeled. Here, the linear model of coregionalization (LMC)<sup>[20]</sup> is used to realize the idea.

Consider a set of latent GP function  $\{f_d(\mathbf{x})\}_{d=1}^D$  with  $\mathbf{x} \in \mathbf{R}^p$ . In the LMC,  $f_d(\mathbf{x})$  can be formulated as

$$f_d(\mathbf{x}) = \sum_{q=1}^Q \sum_{i=1}^{R_q} a_{d,q}^i u_q^i(\mathbf{x}) \quad (8)$$

where the functions  $u_q^i(\mathbf{x})$  is a GP with mean and covariance functions, as shown in Eq.(9), if  $i = i'$  and  $q = q'$ .

$$\text{cov}[u_q^i(\mathbf{x}), u_{q'}^{i'}(\mathbf{x}')] = k_q(\mathbf{x}, \mathbf{x}') \quad (9)$$

For a fixed value of  $\mathbf{x}$ , all the  $f_i(\mathbf{x})$  can be grouped in a vector referred as a vector-valued function shown in

$$\mathbf{f}(\mathbf{x}) = [f_1(\mathbf{x}), f_2(\mathbf{x}), \dots, f_b(\mathbf{x})]^T \quad (10)$$

where  $f_i(\mathbf{x})$  is the  $i$ th output of the vector-valued function  $\mathbf{f}(\mathbf{x})$ . The covariance for  $\mathbf{f}(\mathbf{x})$  is given as

$$\text{cov}[\mathbf{f}(\mathbf{x}), \mathbf{f}(\mathbf{x}')] = \sum_{q=1}^Q \mathbf{A}_q \mathbf{A}_q^T k_q(\mathbf{x}, \mathbf{x}') = \sum_{q=1}^Q \mathbf{B}_q \otimes k_q(\mathbf{x}, \mathbf{x}') \quad (11)$$

where  $\mathbf{A}_q = [\mathbf{a}_q^1, \mathbf{a}_q^2, \dots, \mathbf{a}_q^{R_q}]$ ,  $\otimes$  is the Kronecker product,  $k_q(\mathbf{x}, \mathbf{x}')$  in Fig.5 represents the relationship between input data points, and  $\mathbf{B}_q$  measures the relationship between different latent GPs. The values of non-diagonal elements in  $\mathbf{B}_q$  is positive related to the degree of correlation between different latent GPs.

Based on the mechanical relationship established in Section 2.1, the deformation force can be formulated as

$$\mathbf{F}_{ij} \sim N(F(\sigma_{\text{IRS}}, \sigma_{\text{MSRS},1}, \dots, \sigma_{\text{MSRS},N}), \boldsymbol{\delta}) \quad (12)$$

where  $\mathbf{F}_{ij}$  represents the deformation force measured by fixture  $i$  during machining process  $j$  and  $N$  the Gaussian distribution with a mean function given by the formulated mechanical model;  $\sigma_{\text{IRS}}$  and  $\sigma_{\text{MSRS},i}$  denote the IRS and various MSRS fields, respectively, and  $F(\sigma_{\text{IRS}}, \sigma_{\text{MSRS},1}, \dots, \sigma_{\text{MSRS},N})$  and  $\boldsymbol{\delta}$  the variance.

The process of estimating the IRS and MSRS fields using deformation force is considered as the solution process of the posterior distribution in

$$P(\boldsymbol{\theta} | \mathbf{F}) \quad (13)$$

where  $\boldsymbol{\theta}$  represents all the hyper-parameters in Fig.5 in latent GPs of the estimation process. In cases where the parameter space is extensive, the posterior distribution tends to be high-dimensional and intricate, posing challenges for computation via integration methods. The Markov Chain Monte Carlo (MCMC) method, employed in this paper, is proved to be an efficient approach for addressing posterior probabilities. It accomplishes this by continually evaluating the alignment of the advancing direction with both prior and observed samples, progressively closing in on the proximity of the posterior distribution. After this, an extensive sampling process is conducted within this region of the posterior distribution, leveraging statistical techniques to extract numerical properties of the model.

### 3 A Numerical Example

This paper performs its verification within the FEM framework. To evaluate the feasibility and effectiveness of the proposed method in the inverse problem of residual stress field inference, the infer-

ence error of the proposed method and the TR method based on deformation forces introduced different measurement noises is analyzed, comparing with the theoretical residual stress values.

First, a typical titanium alloy structural component with a size reduction of  $300\text{ mm} \times 100\text{ mm} \times 16\text{ mm}$  was used as the workpiece for validation. The material of the component is Ti6Al4V, with a Young's modulus of 100 GPa and a Poisson's ratio of 0.34. This part includes four groove features, each with a depth of 13.5 mm, a web thickness of 2.5 mm, and a rib thickness of 4 mm. The processing sequence of the slots is illustrated in Fig.7, involving the removal of 9 layers of material from each slot, each with a depth of 1.5 mm. The 10th layer represents the remaining material, with a depth of 2.5 mm. In line with the clamping arrangement within the real machining environment, we establish boundary conditions within the simulation environment. Fixed constraints are applied to the unit nodes corresponding to the secured clamping points on the components. These constraints serve to restrict all six degrees of freedom of the parts, thus maintaining the machining reference point. Additionally, a grounding spring is positioned at the deformation force monitoring point to track deformation forces during the machining process. Following the removal of each layer, four monitoring point sensors record deformation force data, resulting in a total of 36 deformation force data points recorded upon the completion of the machining process.

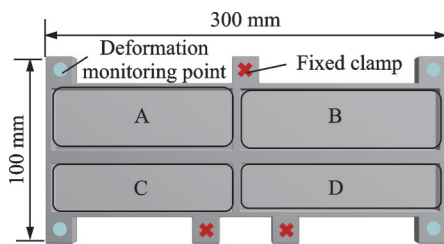


Fig.7 Structural component information

Based on distribution pattern of the IRS and MSRS fields of Ti6Al4V, the IRS field is divided into ten regions. Each layer in  $z$  direction is further divided into a single region, with each region containing  $\sigma_x$ . Additionally, the MSRS field distributed within a depth range of 0.2 mm is divided into five

layers, each layer containing  $\sigma_x$ .

Then, a theoretical RS field distribution is introduced for comparison with inference results, which is based on the research conducted by Fang et al.<sup>[21]</sup> and Outeiro et al.<sup>[22]</sup>, as well as the simulation results presented in this paper. The RS field closely resembles the actual environment, with the IRS symmetrically distributed along the neutral plane of the blank. The radial residual stress ( $\sigma_x, \sigma_y$ ) shares similar distribution characteristics, with tensile stress near the surface layer and compressive stress near the neutral layer, while the axial residual stress ( $\sigma_z$ ) shows relatively uniform distribution. The distribution curve of residual stress on the processing surface exhibits a “√” shape. Under the same machining parameters, the stress levels are linked to the IRS values in the distribution area, a typical feature of the RS distribution in titanium alloy plates.

This paper simplifies the assumption that the distribution of MSRS along the symmetrical region of the neutral plane is the same (Layers 1—4 and 5—8). Consequently, it is inferred that the residual stress field consists of IRS of  $x$  direction in 10 regions and MSRS of  $x$  direction in 25 regions, as shown in Fig.8.

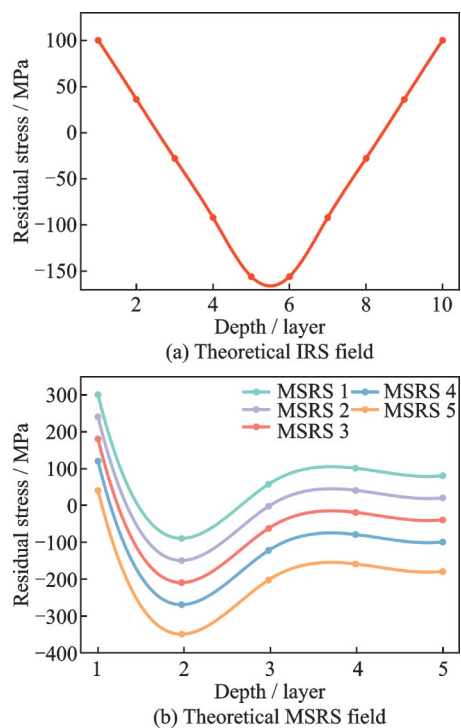


Fig.8 Distribution of theoretical IRS and MSRS fields

To assess the inference effectiveness of the method proposed in this paper in the residual stress field, a real environment is simulated, incorporating measurement errors of 2% and 5% for the calculated deformation forces based on the theoretical RS field, respectively.

The inference results of the IRS and MSRS fields under 2% and 5% noise conditions using the presented GP method and TR method, are depicted in Fig.9 and Fig.10, respectively. The root mean square error (RMSE) of IRS and MSRS inference results using the mentioned methods are compared in Table 2.

As depicted in Fig.9 and Fig.10, the inference outcomes for IRS and MSRS achieved through the presented method exhibit a strong resemblance to the theoretical actual values. In contrast, the trend of IRS alone closely aligns with the theoretical actual values when employing TR method. A compari-

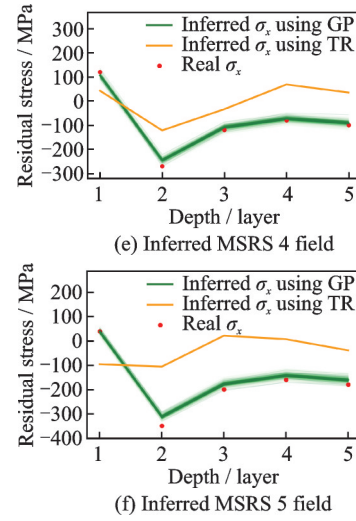
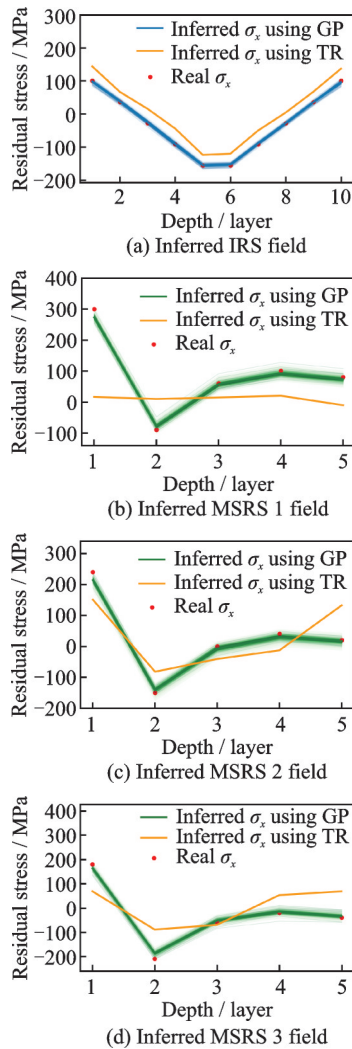
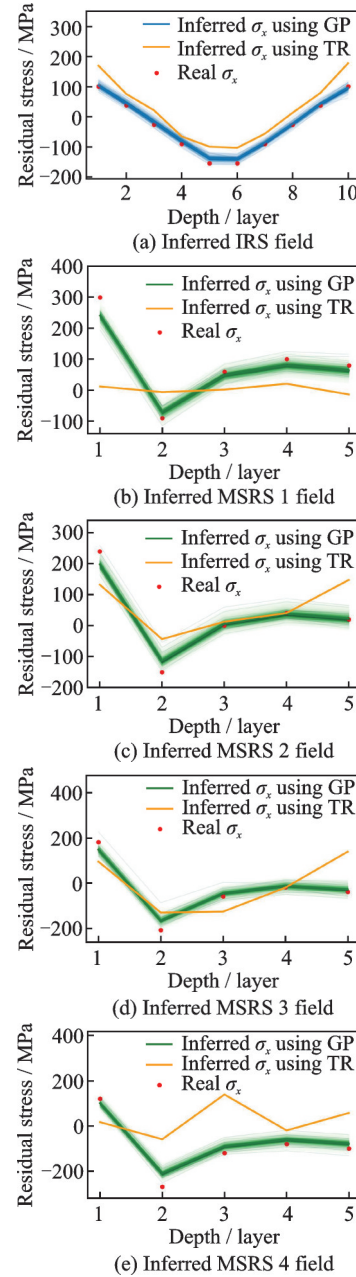


Fig.9 Inference results of RS field under 2% noise condition



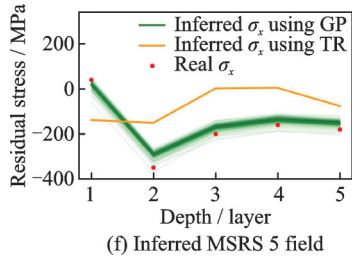


Fig.10 Inference results of RS field under 5% noise condition

**Table 2 RMSE of IRS and MSRS inference results**

Noise/%	IRS_GP/	IRS_TR/	MSRS_GP/	MSRS_TR/
	MPa	MPa	MPa	MPa
2	2.52	37.91	15.52	131.29
5	8.23	50.13	29.31	141.01

son of the RMSE results in Table 2 clearly demonstrates that the inclusion of the correlation prior has markedly enhanced the precision of the inference results. These analytical findings validate the theoretical feasibility of the proposed method, laying the groundwork and providing a robust foundation for subsequent research.

## 4 Conclusions

The feasibility of the presented method is confirmed through simulation data. It is important to note that this study has been validated solely in a three-dimensional simple model with a unidirectional residual stress distribution, while actual parts should consider multi-direction residual stress. More intricate scenarios require thorough analysis. For example, the structures and residual stress field of part are more complex. The measured MSRS values in actual processing experiments can also serve as a prior to further improve the accuracy and reliability of inference results.

We establish an equivalent mechanical model that links IRS and MSRS fields to deformation forces, exploring the correlation between various MSRS distributions under different IRS conditions using FEM in this research. Subsequently, we employ a latent GP within a Bayesian framework to infer IRS and MSRS based on deformation forces.

Based on numerical results of this study, com-

pared with the TR regularization method, using theoretical residual stress as the evaluation index for residual stress field inference error, the inclusion of the correlation prior has markedly enhanced the precision of the inference results, which achieves the purpose of part deformation prediction and control and the fatigue life analysis.

## References

- [1] WANG L, LIU Y, XU H. Review: Recent developments in dynamic load identification for aerospace vehicles considering multi-source uncertainties[J]. Transactions of Nanjing University of Aeronautics and Astronautics, 2021, 38(2): 271-287.
- [2] YANG Y, LI M, LI K R. Comparison and analysis of main effect elements of machining distortion for aluminum alloy and titanium alloy aircraft monolithic component[J]. International Journal of Advanced Manufacturing Technology, 2014, 70 (9/10/11/12): 1803-1811.
- [3] WANG Z, SUN J, CHEN W, et al. Machining distortion of titanium alloys aero engine case based on the energy principles[J]. Metals, 2018, 8(6): 464.
- [4] ZHAO Z, LI Y, LIU C, et al. Predicting part deformation based on deformation force data using physics-informed latent variable model[J]. Robotics and Computer-Integrated Manufacturing, 2021, 72: 102204.
- [5] SRIDHAR B R, DEVANANDA G, RAMACHANDRA K, et al. Effect of machining parameters and heat treatment on the residual stress distribution in titanium alloy IMI-834[J]. Journal of Materials Processing Technology, 2003, 139(1/2/3): 628-634.
- [6] SHAN C, ZHANG M, ZHANG S, et al. Prediction of machining-induced residual stress in orthogonal cutting of Ti6Al4V[J]. The International Journal of Advanced Manufacturing Technology, 2020, 107: 2375-2385.
- [7] CHENG M, JIAO L, YAN P, et al. Prediction of surface residual stress in end milling with Gaussian process regression[J]. Measurement, 2021, 178: 109333.
- [8] YANG Zhen, WANG Yang, WANG Yufeng, et al. Application of 3D mesh dynamic refinement technology in cutting simulation[J]. Journal of Nanjing University of Aeronautics & Astronautics, 2023, 55(1): 80-88. (in Chinese)
- [9] STYGER G, LAUBSCHER R F, OOSTHUIZEN G A. Effect of constitutive modeling during finite element analysis of machining-induced residual stresses in

- Ti6Al4V[J]. *Procedia CIRP*, 2014, 13: 294-301.
- [10] MATHAR J. Determination of inherent stresses by measuring deformations of drilled holes[J]. *Technical Report Archive & Image Library*, 1934, 56(2): 249-254.
- [11] VAIDYANATHAN S, FINNIE I. Determination of residual stresses from stress intensity factor measurements[J]. *Journal of Fluids Engineering*, 1971, 93(2): 242-246.
- [12] WANG S H, ZUO D W, WANG M, et al. Modified layer removal method for measurement of residual stress distribution in thick pre-stretched aluminum plate[J]. *Transactions of Nanjing University of Aeronautics and Astronautics*, 2004, 21(4): 286-290.
- [13] PRIME M B. Cross-sectional mapping of residual stresses by measuring the surface contour after a cut[J]. *Journal of Engineering Materials and Technology*, 2001, 123(2): 162-168.
- [14] GANGULY S, STELMUKH V, FITZPATRICK M E, et al. Use of neutron and synchrotron X-ray diffraction for non-destructive evaluation of weld residual stresses in aluminum alloys[J]. *Journal of Neutron Research*, 2004, 12(1/2/3): 225-231.
- [15] SONG W, XU C, PAN Q, et al. Nondestructive testing and characterization of residual stress field using an ultrasonic method[J]. *Chinese Journal of Mechanical Engineering*, 2016, 29(2): 365-371.
- [16] GOU R, ZHANG Y, XU X, et al. Residual stress measurement of new and in-service X70 pipelines by X-Ray diffraction method[J]. *NDT & E International*, 2011, 44(5): 387-393.
- [17] YUE Q, HE Y, LI Y, et al. Investigation on effects of single- and multiple-pass strategies on residual stress in machining Ti-6Al-4V alloy[J]. *Journal of Manufacturing Processes*, 2022, 77: 272-281.
- [18] DUCOBU F, ARRAZOLA P J, RIVIÈRE-LORPHEVRE E, et al. The CEL method as an alternative to the current modelling approaches for Ti6Al4V orthogonal cutting simulation[J]. *Procedia CIRP*, 2017, 58: 245-250.
- [19] LI Y, GAN W, ZHOU W, et al. Review on residual stress and its effects on manufacturing of aluminium alloy structural panels with typical multi-processes[J]. *Chinese Journal of Aeronautics*, 2023, 36(5): 96-124.
- [20] ÁLVAREZ M A, ROSASCO L, LAWRENCE N D. Kernels for vector-valued functions: A review[J]. *Foundations and Trends in Machine Learning*, 2011, 4(3): 195-266.
- [21] FANG Xiurong, SHAO Yanru, LU Jia, et al. Influence of forging process parameters on residual stress of TC4 titanium alloy forgings[J]. *Forging Technology*, 2021, 46(3): 1-8. (in Chinese)
- [22] OUTEIRO J C, UMBRELLO D, M' SAOUBI R, et al. Evaluation of present numerical models for predicting metal cutting performance and residual stresses[J]. *Machining Science and Technology*, 2015, 19(2): 183-216.

**Acknowledgements** This work was supported by the National Key R&D Program of China (No.2022YFB3402600), the National Science Fund for Distinguished Young Scholars (No.51925505), and the General Program of the National Natural Science Foundation of China (No.52175467).

**Authors** Mr. CHEN Junsong received the B.S. degree in mechanical engineering from Nanjing University of Aeronautics and Astronautics, Nanjing, China, in 2021, where he is currently pursuing the M.S. degree. His research interests are residual stress inference and inverse problem solving.

Prof. LIU Changqing received the B.S., M.S., and Ph.D. degrees from Nanjing University of Aeronautics and Astronautics, Nanjing, China, in 2008, 2011, and 2014, respectively. He has been a professor of Nanjing University of Aeronautics and Astronautics since 2020. His research is focused on data-driven intelligent manufacturing.

**Author contributions** Mr. CHEN Junsong designed the study, compiled the models, conducted the analysis, interpreted the results and wrote the manuscript. Prof. LIU Changqing optimized and improved the overall idea and feasibility of the proposed method. Dr. ZHAO Zhiwei improved the model accuracy and optimized the details of the model. Dr. WANG Wei provided guidance on thesis writing. Dr. XIANG Bingfei and Mr. WEI Zhenkun contributed to the discussion and background of the study. Prof. LI Yingguang contributed to guidance on experimental development. All authors commented on the manuscript draft and approved the submission.

**Competing interests** The authors declare no competing interests.

## 基于潜高斯过程引入理论先验的钛合金结构件残余应力场推断方法

陈俊松<sup>1</sup>, 刘长青<sup>1</sup>, 赵智伟<sup>1</sup>, 王伟<sup>2</sup>, 向兵飞<sup>3</sup>, 危震坤<sup>3</sup>, 李迎光<sup>1</sup>

(1. 南京航空航天大学机电学院, 南京 210016, 中国; 2. 舍夫德大学工程科学学院, 舍夫德, 瑞典;

3. 江西洪都航空工业集团有限责任公司, 南昌 330096, 中国)

**摘要:**残余应力(Residual stress, RS)是导致钛合金结构件加工变形的主要原因。钛合金结构件的残余应力包括初始残余应力(Initial residual stress, IRS)和加工表层残余应力(Machined surface residual stress, MSRS),其中, MSRS是加工表层区域的IRS与高水平的加工残余应力(Machining-induced residual stress, MIRS)耦合作用的结果。结构件的加工变形控制是航空航天工业亟需解决的重要问题,准确获取结构件残余应力场的是加工变形精确预测和控制的基础。然而,现有的残余应力预测方法难以考虑零件制造过程中的各种不确定性,导致预测精度有限。现有的测量方法仅能在样件中测量局部的残余应力,对于大型结构件残余应力场测量,测量效率低。针对以上挑战,本文提出了一种贝叶斯框架下同时推断钛合金结构件IRS和MSRS的方法。该方法将不可观测的IRS和MSRS建模为潜高斯过程,将不同区域的MSRS场之间存在相关性这一先验知识通过具有共享协方差的核函数融入潜高斯过程,并利用可观测的变形力对残余应力场进行推断。本方法提供了一种从概率角度利用变形力数据推断零件残余应力场的有效手段,为后续变形控制策略优化提供了可靠依据。

**关键词:**钛合金;残余应力场推断;潜高斯过程;加工变形